

Convex Clustering through MM: An Efficient Algorithm to Perform Hierarchical Clustering

Daniel J.W. Touw
Patrick J.F. Groenen

*Econometric Institute
Erasmus University Rotterdam
P.O. Box 1738
3000 DR Rotterdam
The Netherlands*

TOUW@ESE.EUR.NL
GROENEN@ESE.EUR.NL

Yoshikazu Terada

*Graduate School of Engineering Science
Osaka University
1-3 Machikaneyama-cho, Toyonaka
Osaka 560-8531, Japan*

TERADA.YOSHIKAZU.ES@OSAKA-U.AC.JP

Abstract

Convex clustering is a modern method with both hierarchical and k -means clustering characteristics. Although convex clustering can capture the complex clustering structure hidden in data, the existing convex clustering algorithms are not scalable to large data sets with sample sizes greater than ten thousand. Moreover, it is known that convex clustering sometimes fails to produce hierarchical clustering structures. This undesirable phenomenon is called cluster split and makes it difficult to interpret clustering results. In this paper, we propose convex clustering through majorization-minimization (CCMM)—an iterative algorithm that uses cluster fusions and sparsity to enforce a complete cluster hierarchy with reduced memory usage. In the CCMM algorithm, the diagonal majorization technique makes a highly efficient update for each iteration. With a current desktop computer, the CCMM algorithm can solve a single clustering problem featuring over one million objects in seven-dimensional space within 70 seconds.

Keywords: convex clustering, convex optimization, hierarchical clustering, majorization-minimization algorithm, unsupervised learning

1. Introduction

Clustering is a core method in unsupervised machine learning and is used in many fields. Applications range from customer segmentation in marketing analytics to object detection in image processing. Over the past two decades, a new method called convex clustering has been introduced that combines aspects of the two popular techniques: k -means (MacQueen, 1967) and hierarchical clustering (see, for example, Gan et al., 2007).

The convex clustering framework was introduced by Pelckmans et al. (2005) who formulated clustering as shrinkage of centroid distances subject to a convex loss function where each p -dimensional object \mathbf{x}_i is represented by its own centroid \mathbf{a}_i . Distance shrinkage is applied to the pairs of \mathbf{a}_i and \mathbf{a}_j using a penalty term, and clusters emerge via the occurrence of equal cluster centroids. Hocking et al. (2011) have explained convex clustering as a convex relaxation of hierarchical clustering, while Lindsten et al. (2011) have staged it as

a convex relaxation of k -means clustering. The common loss function that is considered in these studies is

$$L(\mathbf{A}) = \frac{1}{2} \|\mathbf{X} - \mathbf{A}\|^2 + \lambda \sum_{i < j} w_{ij} \|\mathbf{a}_i - \mathbf{a}_j\|, \quad (1)$$

where \mathbf{A} is a $n \times p$ representation matrix whose rows \mathbf{a}_i^\top are centroids corresponding to objects, w_{ij} is a user-defined nonnegative weight that reflects the importance of clustering objects i and j , \mathbf{X} is the data matrix with rows \mathbf{x}_i^\top , and λ is a penalty-strength parameter that controls the shrinkage of cluster-centroids. Our notation $\|\cdot\|$ denotes either the ℓ_2 -norm of a vector or the Frobenius norm of a matrix. The second term in (1) consists of $\|\mathbf{a}_i - \mathbf{a}_j\|$ representing the Euclidean distance between rows i and j of \mathbf{A} . Each distance is a fusion penalty and behaves like a grouped Lasso (Yuan and Lin, 2006). The minimization of the loss function causes some of these distances $\|\mathbf{a}_i - \mathbf{a}_j\|$ to shrink towards zero, thus interpreted as grouping objects i and j . In related literature, this penalty is often defined using the more general ℓ_q -norm. In this study, we focus on the ℓ_2 -norm since it guarantees a single partitioning of clusters for a given λ .

Without loss of generality, we now assume each column of \mathbf{X} has a mean zero, and we propose a normalized version of (1), that is,

$$L(\mathbf{A}) = \kappa_\epsilon \|\mathbf{X} - \mathbf{A}\|^2 + \lambda \kappa_{\text{pen}} \sum_{i < j} w_{ij} \|\mathbf{a}_i - \mathbf{a}_j\|, \quad (2)$$

where $\kappa_\epsilon = (2\|\mathbf{X}\|^2)^{-1}$ and $\kappa_{\text{pen}} = (\|\mathbf{X}\| \sum_{i < j} w_{ij})^{-1}$. Normalization constants κ_ϵ and κ_{pen} are chosen so that the clustering of the objects in \mathbf{X} , given a particular value of λ , proves invariant to n and p , as well as to the scales of w_{ij} and \mathbf{X} .

One vital property of convex clustering is its strong convexity of the loss function in \mathbf{A} (see the proof in Appendix A). In contrast to k -means, the minimum solution of (2) with a given $\lambda \geq 0$ proves unique, and convex clustering here averts the local minima issue. Additionally, the minimization of the loss function for a sequence of values for λ yields a series of solutions \mathbf{A}_λ that reflects the movement of cluster centroids through the p -dimensional space. These paths are commonly referred to as the *clusterpath* and allow for dynamic visualizations of results (Weylandt et al., 2020). Figure 1a shows a clusterpath that results from minimizing (2) for a data set featuring seven objects in \mathbb{R}^2 . In Figure 1b, these results are converted into a dendrogram—a common visual representation in hierarchical clustering.

Convex clustering incurs several shortcomings. First, Hocking et al. (2011) have noted for particular choices of w_{ij} in (2) that centroids equal for some value λ_1 can reseparate for some value $\lambda_2 > \lambda_1$. This potential violation of cluster hierarchy is undesirable from an interpretative point of view and should be avoided. Second, apart from special focus on the weights, the shapes of clusters recovered by the minimization of (2) tend to be spherical, which is a limiting factor in the application of the method. Third, existing algorithms scale poorly for data sets exceeding a few thousand objects. This study tackles these issues: we develop an algorithm that enforces cluster hierarchy, allows nonconvex cluster-shape retrieval, and is computationally at least 200 times more efficient than state-of-the-art implementations.

The rest of this paper is organized as follows. Section 2 details three different approaches for choosing w_{ij} in (2). We focus on the third (final) choice, sparse weights, to further the

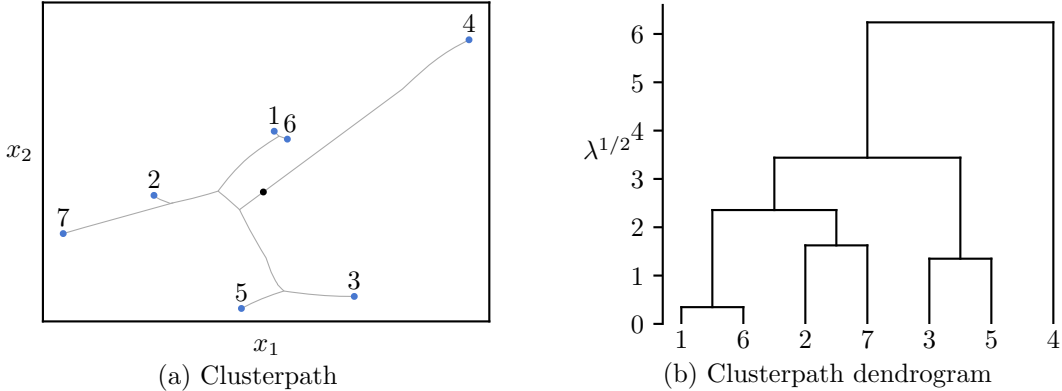


Figure 1: In Panel (a), a clusterpath is computed for seven data points in \mathbb{R}^2 by minimizing (2) for a sequence of values for $\lambda \in [0, 39]$. The objects in the 7×2 data matrix \mathbf{X} are denoted by the blue dots with the paths traced by their cluster centroids in \mathbf{A} appearing in grey. For $\lambda = 39$, the paths of each cluster centroid join at the central black dot. In Panel (b), the corresponding dendrogram appears using the square root of λ as the height where objects are clustered.

understanding of the effect they have on the clusterpath. In Section 3, we combine sparsity and cluster fusions into a majorization-minimization (MM) algorithm to minimize the loss function. Such an iterative algorithm, where a simple optimization problem proxies a more complex problem, aptly converges toward the optimum of the complex problem (Hunter and Lange, 2004). We dub this resulting algorithm *convex clustering through majorization-minimization* (CCMM). In Sections 4 and 5, we present results of the simulation study and conclude our paper.

2. Hierarchy and Weights in Convex Clustering

One potential pitfall of convex clustering is that increasing λ does not always guarantee a complete cluster hierarchy. In this section, we offer a solution for this. To make convex clustering scalable for big n , sparsity of weights is necessary where many w_{ij} are set to zero. Sun et al. (2021) have shown that using such sparsity in weights equips their method to minimize a single instance of (2) in roughly six minutes for a data set of 200,000 objects. However, under such extreme sparsity, it is likely that some groups of objects are not connected to the remaining objects via nonzero weights. Consequently, the original convex clustering problem can be reduced to separate optimization problems. It is this reducibility that renders a complete cluster hierarchy impossible. Here, we provide a formal proof of this property and craft a solution that has minimal impact on the scalability of our algorithm.

2.1 Enforcing Hierarchical Clusters

To address cluster splits, we first note that Hocking et al. (2011) conjectured that splits do not occur when weights w_{ij} are nonincreasing in $\|\mathbf{x}_i - \mathbf{x}_j\|$. This has been empirically confirmed by Chi and Lange (2015) and Weylandt et al. (2020), as well as in our research. Therefore, if the weights satisfy this condition, we can fuse the rows of \mathbf{A} where $\|\mathbf{a}_i - \mathbf{a}_j\| = 0$ and store all unique centroids in $c \times p$ matrix \mathbf{M} . We next define $n \times c$ cluster membership

matrix \mathbf{U} as having elements

$$u_{ik} = \begin{cases} 1 & \text{if object } i \text{ belongs to cluster } k, \text{ and} \\ 0 & \text{otherwise,} \end{cases}$$

and denote row i of \mathbf{U} by row vector \mathbf{u}_i^\top and column k by column vector \mathbf{u}_k . Instead of minimizing (2) with respect to \mathbf{A} , we perform minimization on \mathbf{M} and continue the fusion process whenever $\|\mathbf{m}_k - \mathbf{m}_l\| = 0$. The matrix \mathbf{A} can be retrieved simply via $\mathbf{A} = \mathbf{U}\mathbf{M}$.

We propose preventing any merged clusters from splitting, thereby ensuring a hierarchy of clusters with increasing λ . This strategy also yields a substantial gain in computational efficiency since \mathbf{M} has fewer rows than \mathbf{A} .

2.2 Introducing Sparsity

In existing literature, three general approaches for choosing the weights can be identified. The first type, used by Pelckmans et al. (2005) and Lindsten et al. (2011), simply sets all $w_{ij} = 1$ in a unit-weights approach. However, using convex clustering in combination with unit weights leads to quite poor clustering performance. This is illustrated by the clusterpath in Figure 2a where almost no clustering takes place before each individual path reaches the center. Hocking et al. (2011) have found that weights that decrease in the distance between \mathbf{x}_i and \mathbf{x}_j allow for better cluster recovery. They suggest using weights proportional to the Gaussian distribution: $w_{ij} = \exp(-\psi\|\mathbf{x}_i - \mathbf{x}_j\|^2)$ with hyperparameter ψ scaling these high-dimensional Euclidean distances.

Figure 2b shows that Gaussian weights indeed outperform unit weights in terms of clustering, but fail in allowing recovery of the original two interlocking half moons. Finally, as an extension to Gaussian weights, Chi and Lange (2015) set w_{ij} to zero when object i is not among the k nearest neighbors of j . This approach improves clustering performance (see Figure 2c) with the added advantage of greatly reducing the computational complexity of minimization algorithms. In this paper, a scaled version of the k -nn Gaussian weights is used to ensure that weights remain unaffected by the scale of the data, yielding the following representation of the sparse weight matrix \mathbf{W}

$$w_{ij} = w_{ji} = \begin{cases} \exp\left(-\phi \frac{\|\mathbf{x}_i - \mathbf{x}_j\|^2}{\text{mean}_{i',j'} \|\mathbf{x}_{i'} - \mathbf{x}_{j'}\|^2}\right) & \text{if } j \in \mathcal{S}_i^{(k)} \vee i \in \mathcal{S}_j^{(k)} \\ 0 & \text{otherwise,} \end{cases} \quad (3)$$

where $\mathcal{S}_i^{(k)}$ denotes the set of k nearest neighbors of i , $\phi \geq 0$ is a tuning parameter, and $\|\mathbf{x}_i - \mathbf{x}_j\|^2$ is scaled by the mean of all squared distances.

2.3 Enforcing Irreducibility

Weight sparsity can improve the flexibility of convex clustering and slash computation time. However, sparsity also incurs a new challenge: the emergence of different groups of objects, for example \mathcal{C}_k and \mathcal{C}_l where $w_{ij} = 0$ for all $i \in \mathcal{C}_k$ and $j \in \mathcal{C}_l$, that trigger reducibility of the convex clustering problem where a loss function can split into standalone sub-problems. Such a \mathbf{W} we call ‘‘disconnected’’ per the corresponding disconnected graph in graph theory. The theorem below presents irreducibility (connectedness) of \mathbf{W} as a sufficient condition for a clusterpath ending in a single partition.

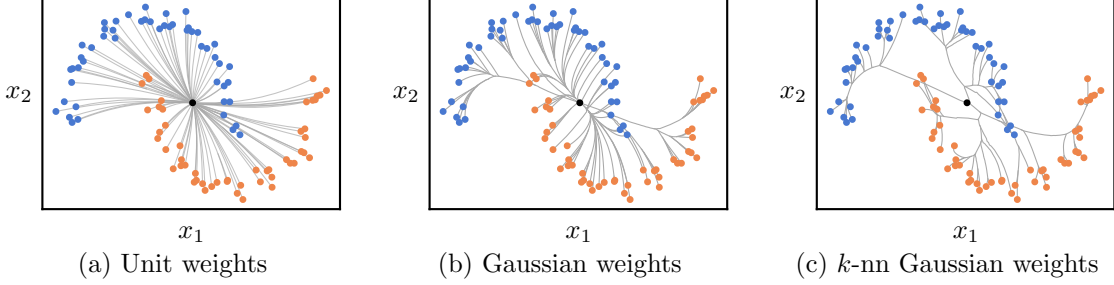


Figure 2: Comparison of three clusterpaths computed for the same data using unit weights in the penalty for Panel (a), Gaussian weights with $\phi = 4$ for Panel (b), and k -nn Gaussian weights with $k = 10$ and $\phi = 4$ for Panel (c). A black dot marks the location of the final cluster in each clusterpath.

Theorem 1 *If \mathbf{W} is connected, then for some sufficiently large, finite value of λ , a global minimum of (2) exists where all rows of the solution \mathbf{A} are identical to the mean of the rows in \mathbf{X} .*

This theorem is a more general version of Proposition 1 in Pelckmans et al. (2005), and we provide the proof in Appendix B. Using Theorem 1, we can determine what happens if \mathbf{W} is disconnected as formalized in the following corollary.

Corollary 2 *Let $\mathbf{A}_{\mathcal{C}_k}$ be the $|\mathcal{C}_k| \times p$ matrix that results from selecting only rows $i \in \mathcal{C}_k$ from \mathbf{A} , and let $\mathbf{W}_{\mathcal{C}_k}$ be the $|\mathcal{C}_k| \times |\mathcal{C}_k|$ matrix that results from selecting only rows $i \in \mathcal{C}_k$ and columns $j \in \mathcal{C}_k$ from \mathbf{W} where $|\mathcal{C}_k| = \mathbf{1}^\top \mathbf{u}_k$ denotes the size of cluster k . If \mathbf{W} is disconnected, the convex clustering problem can disaggregate into K separate clustering problems where a sufficiently large, finite value for λ minimizes each problem via $\mathbf{A}_{\mathcal{C}_k} = \mathbf{1}\bar{\mathbf{x}}_k^\top$. Here, \mathcal{C}_k comprise the K subsets of objects where $\mathbf{W}_{\mathcal{C}_k}$ is connected and $\mathbf{W}_{\mathcal{C}_k \cup \mathcal{C}_l}$ is disconnected for any $k \neq l$, and $\bar{\mathbf{x}}_k$ is the mean of \mathbf{x}_i for $i \in \mathcal{C}_k$.*

Proof For disconnected \mathbf{W} , the loss function $L(\mathbf{A})$ equates the sum of K distinct loss functions:

$$\begin{aligned} L(\mathbf{A}) &= \kappa_\epsilon \sum_{i=1}^n \|\mathbf{x}_i - \mathbf{a}_i\|^2 + \lambda \kappa_{\text{pen}} \sum_{i < j} w_{ij} \|\mathbf{a}_i - \mathbf{a}_j\| \\ &= \sum_{k=1}^K \left[\kappa_\epsilon \sum_{i \in \mathcal{C}_k} \|\mathbf{x}_i - \mathbf{a}_i\|^2 + \lambda \kappa_{\text{pen}} \sum_{\substack{i, j \in \mathcal{C}_k \\ i < j}} w_{ij} \|\mathbf{a}_i - \mathbf{a}_j\| \right]. \end{aligned}$$

The minimum of this sum is obtained by independently minimizing each sub-problem. Following Theorem 1, the rows of $\mathbf{A}_{\mathcal{C}_k}$ can be computed as $\mathbf{a}^{(k)} = |\mathcal{C}_k|^{-1} \sum_{i \in \mathcal{C}_k} \mathbf{x}_i = \bar{\mathbf{x}}_k$ for sufficiently large λ . \blacksquare

Since the sparse specification of \mathbf{W} in (3) does not guarantee a connected weight matrix, Theorem 1 and Corollary 2 indicate that it may be impossible to obtain a single cluster when performing convex clustering for large λ . Still, hierarchical clustering methods require

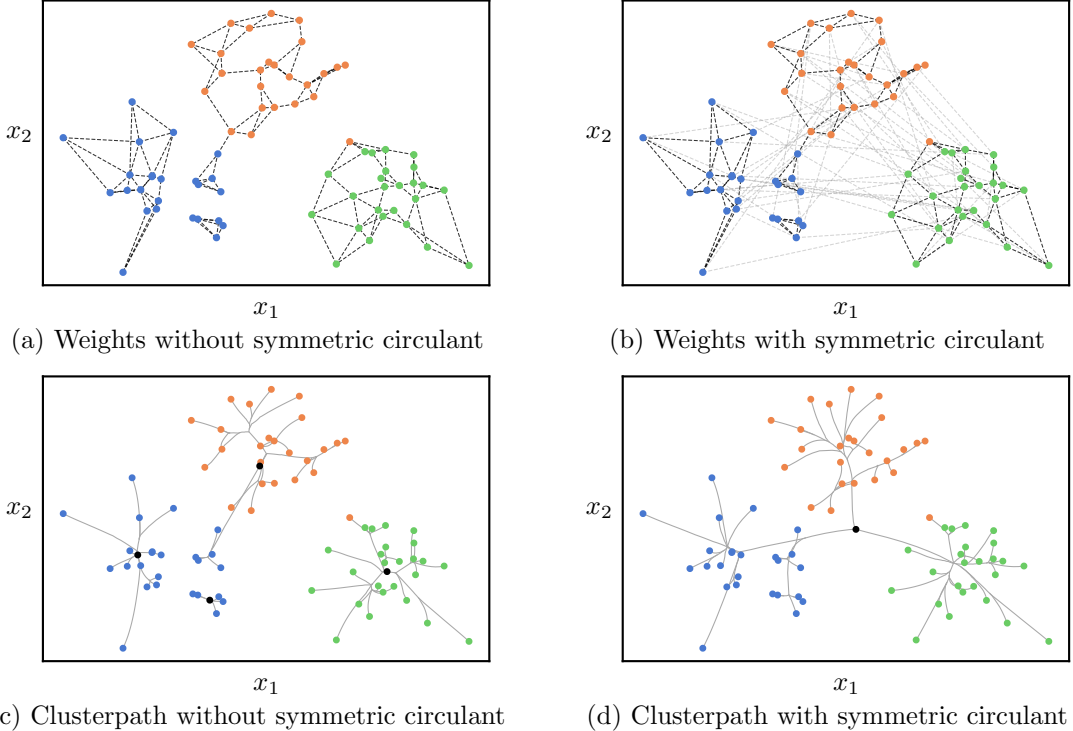


Figure 3: The effect of the use of a symmetric circulant matrix to ensure connectedness of the weight matrix on convex clustering. In Panel (a), two objects are connected by an edge if their weight as determined by (3) is nonzero and two objects are connected by an edge in Panel (b) if their weight as determined by (4) is nonzero. In both cases $k = 3$ is used. The additional edges that are added due to the symmetric circulant matrix are indicated by light grey dashed lines. The clusterpaths that result from convex clustering with the two different weight matrices are shown in panels (c) and (d). The colors indicate the true clusters according to the data generating process and the black dot the location of the final cluster(s) in each clusterpath.

all objects to eventually merge into a single cluster. To attain a single-cluster result from convex clustering using a sparse weight matrix, connectedness of \mathbf{W} must be guaranteed.

To do so, we propose adding nonzero weights to the sparse weight matrix \mathbf{W} to ensure its connectedness. To avoid expensive pre-processing steps, we enlist a symmetric circulant matrix to provide a rule for adding non-zero entries to \mathbf{W} . A symmetric circulant is a square matrix \mathbf{H} where each row is identical to the row above, but shifted one position to the right and satisfying $h_{ij} = h_{ji}$ (Gower and Groenen, 1991). One example of the most sparse symmetric circulant *not* forming the identity matrix for $n = 6$ is

$$\mathbf{H} = \begin{bmatrix} 0 & 1 & 0 & 0 & 0 & 1 \\ 1 & 0 & 1 & 0 & 0 & 0 \\ 0 & 1 & 0 & 1 & 0 & 0 \\ 0 & 0 & 1 & 0 & 1 & 0 \\ 0 & 0 & 0 & 1 & 0 & 1 \\ 1 & 0 & 0 & 0 & 1 & 0 \end{bmatrix}.$$

As a weight matrix, \mathbf{H} is connected by definition. Therefore, if nonzero weights are added to \mathbf{W} according to the nonzero elements of \mathbf{H} , connectedness of \mathbf{W} is guaranteed while adding no more than n nonsparse elements. In a graphical context, Figure 3a features nonzero weights based on three nearest neighbors as edges between objects in a generated data set. In Figure 3b, the additional nonzero weights per the symmetric circulant matrix appear in light grey. The new formulation of the weight matrix is

$$w_{ij} = w_{ji} = \begin{cases} \exp\left(-\phi \frac{\|\mathbf{x}_i - \mathbf{x}_j\|^2}{\text{mean}_{i',j'}(\|\mathbf{x}_{i'} - \mathbf{x}_{j'}\|^2)}\right) & \text{if } j \in \mathcal{S}_i^{(k)} \vee i \in \mathcal{S}_j^{(k)} \vee h_{ij} = 1, \\ 0 & \text{otherwise.} \end{cases} \quad (4)$$

Figure 3 also depicts the effect of \mathbf{W} on the clusterpaths that result from minimizing (2). In Figure 3c, the disconnected \mathbf{W} from (3), using only k -nn, fails to produce a clusterpath leading to a complete hierarchy. In contrast, the combination of k -nn and a symmetric circulant in (4) produces a \mathbf{W} which nicely produces a complete hierarchy (see Figure 3d).

The exact level of sparsity depends on the data. The k -nn relation is not symmetric, and enforcement of symmetry in (3) and (4) can vary the number of nonzero weights. An upper bound for the number of non-sparse elements following (3) is kn , then increased to $(k + 1)n$ when ensuring connectedness via a symmetric circulant matrix in (4). This contrasts with the dense specification of \mathbf{W} always demanding the storage of $n(n - 1)/2$ weights that proves quadratic in n .

3. Minimization Algorithm

Cluster fusions play an important role in the CCMM algorithm by ensuring that no cluster splits occur while reducing the computational burden. Therefore, we first show in Section 3.1 how fusions are enlisted to formulate the loss function in terms of the unique centroids in matrix \mathbf{A} . In Section 3.2, a surrogate function based on the reformulated loss function is derived that can be minimized analytically in linear time—making it an excellent candidate for an iterative minimization algorithm. In Section 3.3, we present the complete CCMM algorithm and discuss some of its properties.

3.1 Cluster Fusions

To avoid cluster splits and to reduce the computational burden, rows of \mathbf{A} that are identical can be merged as proposed by Hocking et al. (2011). This approach tracks all unique rows of \mathbf{A} and stores them in the $c \times p$ matrix \mathbf{M} where c denotes the number of unique rows or, equivalently, the current number of clusters. The decision to fuse two clusters is based on whether \mathbf{m}_k and \mathbf{m}_l are sufficiently close given some threshold ε_f . If $\|\mathbf{m}_l - \mathbf{m}_k\| \leq \varepsilon_f$ for some $k \neq l$, then rows \mathbf{m}_k and \mathbf{m}_l in \mathbf{M} are replaced by the weighted average

$$\mathbf{m}_{new} = \frac{|C_k|\mathbf{m}_k + |C_l|\mathbf{m}_l}{|C_k| + |C_l|}. \quad (5)$$

If \mathbf{UM} replaces \mathbf{A} , we can rewrite the loss function in (2) in terms of \mathbf{M} . As stated earlier, the advantage here is that the complexity of computing an update for \mathbf{M} in an iterative algorithm no longer scales in the number of objects n , but in the number of clusters c

ranging from n to 1. The new loss function becomes

$$\begin{aligned} L(\mathbf{M}) &= \kappa_\epsilon \|\mathbf{X} - \mathbf{U}\mathbf{M}\|^2 + \lambda \kappa_{\text{pen}} \sum_{i < j} w_{ij} \|\mathbf{u}_i^\top \mathbf{M} - \mathbf{u}_j^\top \mathbf{M}\| \\ &= \kappa_\epsilon \|\mathbf{X} - \mathbf{U}\mathbf{M}\|^2 + \lambda \kappa_{\text{pen}} \sum_{k < l} \mathbf{u}_k^\top \mathbf{W} \mathbf{u}_l \|\mathbf{m}_k - \mathbf{m}_l\|. \end{aligned} \quad (6)$$

However, since ε_f is a value near zero, \mathbf{m}_k and \mathbf{m}_l may not equate, thus yielding a difference between $L(\mathbf{M})$ and the $L(\mathbf{M}_{\text{new}})$ that results from fusing \mathbf{m}_k and \mathbf{m}_l . The following theorem states that as ε_f approaches zero, so does $|L(\mathbf{M}) - L(\mathbf{M}_{\text{new}})|$. The proof is in Appendix C.

Theorem 3 *Let the matrix \mathbf{M} contain the c unique rows of \mathbf{A} , and let ε_f be the threshold used for fusing rows of \mathbf{M} . Assume that $\|\mathbf{m}_k - \mathbf{m}_l\| \leq \varepsilon_f$ for some $k \neq l$. Let \mathbf{m}_{new} be the weighted average of \mathbf{m}_k and \mathbf{m}_l computed as in (5), and let \mathbf{M}_{new} be the matrix that results from setting \mathbf{m}_k and \mathbf{m}_l to \mathbf{m}_{new} . Then, for fixed λ and \mathbf{W} , the absolute error $|L(\mathbf{M}) - L(\mathbf{M}_{\text{new}})|$ tends toward zero as $\varepsilon_f \rightarrow 0$.*

An important consequence of Theorem 3 is that for sufficiently small ε_f there are no order effects of fusing two rows of \mathbf{M} .

3.2 Majorization-Minimization Update

To minimize the loss function in (6), we enlist MM. Here, an objective function difficult to minimize is replaced by a simpler or surrogate function with a minimum that can be computed analytically. A similar procedure was first described by Weiszfeld (1937), but Ortega and Rheinboldt (1970) were the first to apply it in the context of a line search. Later, it was developed as a general minimization method by independently by De Leeuw (1977) and Voß and Eckhardt (1980). In machine learning literature, MM is also known as the concave-convex procedure (CCCP; Yuille and Rangarajan, 2003). Additional examples can be found in Lange et al. (2000) and Hunter and Lange (2004).

MM exploits a majorization function that touches the target function at a “supporting” point and that is never exceeded by the target function over its domain. Let $g(\mathbf{M}, \mathbf{M}_0)$ denote this majorization function with \mathbf{M}_0 as the supporting point. The criteria can be summarized as

$$g(\mathbf{M}, \mathbf{M}_0) \geq L(\mathbf{M}) \quad \text{and} \quad g(\mathbf{M}_0, \mathbf{M}_0) = L(\mathbf{M}_0).$$

The key is to choose a function for $g(\mathbf{M}, \mathbf{M}_0)$ that is quadratic in \mathbf{M} where its minimum can be computed analytically for use in the next iteration as the new supporting point, thus converging toward a minimum of the target function. If the target function is strictly convex and coercive, this is the unique minimum (see, for example, Boyd and Vandenberghe, 2004).

The first step in defining $g(\mathbf{M}, \mathbf{M}_0)$ is to majorize the ℓ_2 -norm of the differences between rows of \mathbf{M} . If $a, b \geq 0$, then $(ab)^{1/2} \leq (a + b)/2$ since $0 \leq (a^{1/2} - b^{1/2})^2$. Substituting $a = \|\boldsymbol{\theta}\|^2$ and $b = \|\boldsymbol{\theta}_0\|^2$ yields

$$\|\boldsymbol{\theta}\| \leq \frac{1}{2} \frac{\|\boldsymbol{\theta}\|^2}{\|\boldsymbol{\theta}_0\|} + \frac{1}{2} \|\boldsymbol{\theta}_0\|, \quad (7)$$

for $\|\boldsymbol{\theta}_0\| > 0$. Applying this inequality to $\|\mathbf{m}_k - \mathbf{m}_l\|$, using $\|\mathbf{m}_k - \mathbf{m}_l\|^2 = (\mathbf{m}_k - \mathbf{m}_l)^\top (\mathbf{m}_k - \mathbf{m}_l) = \text{tr}(\mathbf{m}_k - \mathbf{m}_l)(\mathbf{m}_k - \mathbf{m}_l)^\top = \text{tr} \mathbf{M}^\top \mathbf{E}_{kl} \mathbf{M}$ subject to $\mathbf{E}_{kl} = (\mathbf{e}_k - \mathbf{e}_l)(\mathbf{e}_k - \mathbf{e}_l)^\top$ with \mathbf{e}_k being the k^{th} column of the $c \times c$ identity matrix, finally yields

$$\begin{aligned} L(\mathbf{M}) &\leq \kappa_\epsilon \|\mathbf{X} - \mathbf{U}\mathbf{M}\|^2 + \frac{\lambda\kappa_{\text{pen}}}{2} \sum_{k < l} \mathbf{u}_k^\top \mathbf{W} \mathbf{u}_l \left(\frac{\|\mathbf{m}_k - \mathbf{m}_l\|^2}{\|\mathbf{m}_{0,k} - \mathbf{m}_{0,l}\|} + \|\mathbf{m}_{0,k} - \mathbf{m}_{0,l}\| \right) \\ &= \kappa_\epsilon \|\mathbf{X} - \mathbf{U}\mathbf{M}\|^2 + \frac{\lambda\kappa_{\text{pen}}}{2} \text{tr} \mathbf{M}^\top \mathbf{C}_0 \mathbf{M} + c(\mathbf{M}_0), \end{aligned} \quad (8)$$

where

$$\mathbf{C}_0 = \sum_{k < l} \frac{\mathbf{u}_k^\top \mathbf{W} \mathbf{u}_l}{\|\mathbf{m}_{0,k} - \mathbf{m}_{0,l}\|} \mathbf{E}_{kl},$$

with $c(\mathbf{M}_0)$ the collection of constant terms not depending on \mathbf{M} . We should note that using cluster fusions in the algorithm prevents a division by zero in the computation of \mathbf{C}_0 .

At this point, the function in (8) is quadratic in \mathbf{M} and is continuously differentiable, aptly suiting it for use as $g(\mathbf{M}, \mathbf{M}_0)$ in the MM algorithm. Here, the update for \mathbf{M} satisfies

$$\begin{aligned} \frac{\partial g(\mathbf{M}, \mathbf{M}_0)}{\partial \mathbf{M}} &= 2\kappa_\epsilon \mathbf{U}^\top \mathbf{U} \mathbf{M} - 2\kappa_\epsilon \mathbf{U}^\top \mathbf{X} + \lambda\kappa_{\text{pen}} \mathbf{C}_0 \mathbf{M} = \mathbf{0} \\ &\quad \left(\mathbf{U}^\top \mathbf{U} + \frac{\lambda\kappa_{\text{pen}}}{2\kappa_\epsilon} \mathbf{C}_0 \right) \mathbf{M} = \mathbf{U}^\top \mathbf{X}, \end{aligned} \quad (9)$$

where $\mathbf{0}$ is a matrix of zeroes. However, solving the system of equations in (9) incurs a complexity of $\mathcal{O}(c^3)$ —a costly operation when c is large. As $\mathbf{U}^\top \mathbf{U}$ is a diagonal matrix, the issue lies with the matrix \mathbf{C}_0 . We thus take another step in the majorization process by eliminating $\text{tr} \mathbf{M}^\top \mathbf{C}_0 \mathbf{M}$ from (8). Groenen et al. (1999) treated a similar problem by carrying out a majorization step using upper the bounds of the eigenvalues of \mathbf{C}_0 . If \mathbf{D}_0 is a diagonal matrix that features these upper bounds as its elements, then $\mathbf{D}_0 - \mathbf{C}_0$ is positive semi-definite. Consequently, the following inequality can be derived

$$\begin{aligned} 0 &\leq \text{tr}[(\mathbf{M} - \mathbf{M}_0)^\top (\mathbf{D}_0 - \mathbf{C}_0)(\mathbf{M} - \mathbf{M}_0)] \\ \text{tr} \mathbf{M}^\top \mathbf{C}_0 \mathbf{M} &\leq \text{tr} \mathbf{M}^\top \mathbf{D}_0 \mathbf{M} - 2 \text{tr} \mathbf{M}^\top (\mathbf{D}_0 - \mathbf{C}_0) \mathbf{M}_0 + \text{tr} \mathbf{M}_0^\top (\mathbf{D}_0 - \mathbf{C}_0) \mathbf{M}_0. \end{aligned}$$

To obtain \mathbf{D}_0 , Gershgorin's Circle Theorem (Bronson, 1989) can be used where eigenvalues of \mathbf{C}_0 fall within $[c_{kk} - \sum_{l \neq k} |c_{kl}|, c_{kk} + \sum_{l \neq k} |c_{kl}|]$. Due to the structure of \mathbf{C}_0 , the upper bound $c_{kk} + \sum_{l \neq k} |c_{kl}| = 2c_{kk}$, which means that \mathbf{D}_0 can be computed as twice the diagonal of \mathbf{C}_0 . Substituting the inequality for $\text{tr} \mathbf{M}^\top \mathbf{C}_0 \mathbf{M}$ into the majorized loss function in (8) yields

$$\begin{aligned} L(\mathbf{M}) &\leq \kappa_\epsilon \|\mathbf{X} - \mathbf{U}\mathbf{M}\|^2 + \frac{\lambda\kappa_{\text{pen}}}{2} \text{tr} \mathbf{M}^\top \mathbf{D}_0 \mathbf{M} - \lambda\kappa_{\text{pen}} \text{tr} \mathbf{M}^\top (\mathbf{D}_0 - \mathbf{C}_0) \mathbf{M}_0 + c(\mathbf{M}_0) \\ &= g(\mathbf{M}, \mathbf{M}_0). \end{aligned}$$

Then, the matrix \mathbf{M} that minimizes $g(\mathbf{M}, \mathbf{M}_0)$ can be computed as

$$\frac{\partial g(\mathbf{M}, \mathbf{M}_0)}{\partial \mathbf{M}} = 2\kappa_\epsilon \mathbf{U}^\top \mathbf{U} \mathbf{M} - 2\kappa_\epsilon \mathbf{U}^\top \mathbf{X} + \lambda\kappa_{\text{pen}} (\mathbf{D}_0 \mathbf{M} - (\mathbf{D}_0 - \mathbf{C}_0) \mathbf{M}_0) = \mathbf{0}$$

$$\mathbf{M} = \left(\mathbf{U}^\top \mathbf{U} + \frac{\lambda \kappa_{\text{pen}}}{2\kappa_\epsilon} \mathbf{D}_0 \right)^{-1} \left(\mathbf{U}^\top \mathbf{X} + \frac{\lambda \kappa_{\text{pen}}}{2\kappa_\epsilon} (\mathbf{D}_0 - \mathbf{C}_0) \mathbf{M}_0 \right). \quad (10)$$

Note that the first term is a diagonal matrix with elements

$$\left(\mathbf{U}^\top \mathbf{U} + \frac{\lambda \kappa_{\text{pen}}}{2\kappa_\epsilon} \mathbf{D}_0 \right)_{kk}^{-1} = \left(|\mathcal{C}_k| + \frac{\lambda \kappa_{\text{pen}}}{2\kappa_\epsilon} d_{0,kk} \right)^{-1}$$

that will now permit straightforward updates. In Section 3.3, we present the complete algorithm that uses this update to perform convex clustering.

3.3 Implementation

In Algorithm 1, we present the CCMM algorithm used to minimize (6). The algorithm is divided into six steps, each performing a straightforward task. Step 1 initializes several variables used in the minimization. Notable are $\tilde{\mathbf{X}}$ and $\tilde{\mathbf{W}}$ used to track $\mathbf{U}^\top \mathbf{X}$ and $\mathbf{U}^\top \mathbf{WU}$ to avoid unnecessary computations. The main loop of the algorithm starts by computing the update per (10) in Step 2. To reduce the number of iterations required to reach convergence, we make use of a relaxed update (De Leeuw and Heiser, 1980), which we call “step doubling.” When step doubling, the update for \mathbf{M} is computed as $2\mathbf{M}_1 - \mathbf{M}_0$, where \mathbf{M}_1 is the result from Step 2 and \mathbf{M}_0 the supporting point. In practice, this type of update is applied after a number of burn-in iterations b to avoid “stepping over” the minimum. This accelerated update is computed in Step 3, and in our experiments we typically set b to 25.

In Step 4, rows in \mathbf{M}_0 are fused. As Hocking et al. (2011) have noted, the ideal approach for determining fusions would be to evaluate the change in loss function per centroid pair. However, this may not be viable when it incurs a large number of additional computations. Therefore, the authors suggest using a threshold that triggers a cluster fusion when $\|\mathbf{m}_k - \mathbf{m}_l\| \leq \varepsilon_f$. We propose a formulation of ε_f that reflects the scale of the data while also securing a threshold not too small in cases of very similar (duplicate) objects. Here, ε_f computes as

$$\varepsilon_f = \tau \text{median}_{i,j} (\|\mathbf{x}_i - \mathbf{x}_j\|), \quad (11)$$

where τ denotes a specified fraction of the median of Euclidean distances between objects. For very large data sets, the median of medians may estimate this value. In our experiments, we typically set τ to 10^{-3} . The fusion process outputs the $c_{\text{old}} \times c_{\text{new}}$ membership matrix \mathbf{U}_{new} that maps the old clusters to the new ones. This matrix can be used to update $\tilde{\mathbf{X}}$ and $\tilde{\mathbf{W}}$ as $\mathbf{U}_{\text{new}}^\top \tilde{\mathbf{X}}$ and $\mathbf{U}_{\text{new}}^\top \tilde{\mathbf{W}} \mathbf{U}_{\text{new}}$, respectively. Additionally, Step 4 repeats if there are rows in the updated matrix \mathbf{M}_0 for which $\|\mathbf{m}_k - \mathbf{m}_l\| \leq \varepsilon_f$.

In Step 5, the loss function value is updated. When the relative decrease in the loss exceeds some value ε_c , the algorithm reverts to Step 2. At convergence, the resulting matrix \mathbf{A} is computed and returned to the user. For the results presented in this paper, we set the value of ε_c to 10^{-6} . Finally, when computing a clusterpath for multiple values of λ , warm starts can be used by setting \mathbf{M}_0 to the solution of the minimization for the previous value of λ in Step 1.

To analyze algorithmic complexity, we focus on two of the six steps. First, in Step 2, the update derived in (10) is computed. A key feature of this update is that it can be done in a single loop over the nonzero elements of the $c \times c$ matrix $\tilde{\mathbf{W}}$. Hence, this step has a

Algorithm 1: Convex clustering through majorization-minimization (CCMM).

Key parts of the algorithm are Step 2 where the update derived in (10) is computed, and Step 4 where cluster fusions are performed. Step 3 is executed only after a number of burn-in iterations to accelerate convergence. Remaining steps perform initializations and bookkeeping.

Input: \mathbf{X} , \mathbf{W} , λ , ε_c , ε_f , b

Output: \mathbf{A}

```

 $\mathbf{M}_0 := \mathbf{X}$  ▷ Step 1
 $\mathbf{U} := \mathbf{I}_n$ 
 $L_1 := L(\mathbf{M}_0)$ 
 $L_0 := (1 + 2\varepsilon_c)L_1$ 
 $\tilde{\mathbf{X}} := \mathbf{X}$ 
 $\tilde{\mathbf{W}} := \mathbf{W}$ 
 $\kappa_\epsilon := (2\|\mathbf{X}\|^2)^{-1}$ 
 $\kappa_{\text{pen}} := (\|\mathbf{X}\| \sum_{i < j} w_{ij})^{-1}$ 
 $\gamma := \lambda \kappa_{\text{pen}} / (2\kappa_\epsilon)$ 
 $t := 1$ 

while  $(L_0 - L_1)/L_1 > \varepsilon_c$  do
     $\mathbf{C}_0 := \sum_{k=2}^c \sum_{l=1}^{k-1} (\tilde{w}_{kl} / \|\mathbf{m}_{0,k} - \mathbf{m}_{0,l}\|) \mathbf{E}_{kl}$  ▷ Step 2
     $\mathbf{D}_0 := \text{diag}(\mathbf{C}_0)$ 
     $\mathbf{M}_1 := (\mathbf{U}^\top \mathbf{U} + \gamma \mathbf{D}_0)^{-1} (\tilde{\mathbf{X}} + \gamma(\mathbf{D}_0 - \mathbf{C}_0) \mathbf{M}_0)$ 
    if  $t > b$  then ▷ Step 3
         $\mathbf{M}_0 := 2\mathbf{M}_1 - \mathbf{M}_0$ 
    else
         $\mathbf{M}_0 := \mathbf{M}_1$ 
    while  $\exists(k, l) : \|\mathbf{m}_{0,k} - \mathbf{m}_{0,l}\| \leq \varepsilon_f$  do ▷ Step 4
        Fuse rows of  $\mathbf{M}_0$  and obtain  $\mathbf{U}_{\text{new}}$ 
         $\tilde{\mathbf{X}} := \mathbf{U}_{\text{new}}^\top \tilde{\mathbf{X}}$ 
         $\tilde{\mathbf{W}} := \mathbf{U}_{\text{new}}^\top \tilde{\mathbf{W}} \mathbf{U}_{\text{new}}$ 
         $\mathbf{U} := \mathbf{U} \mathbf{U}_{\text{new}}$ 
     $L_0 := L_1$  ▷ Step 5
     $L_1 := L(\mathbf{M}_0)$ 
     $t := t + 1$ 
A :=  $\mathbf{U} \mathbf{M}_0$  ▷ Step 6

```

complexity of $\mathcal{O}(npk)$ where n is an upper bound on c . Second, in Step 4, the rows of \mathbf{M}_0 fuse, and several matrices update. Using the nonzero elements of $\widetilde{\mathbf{W}}$, a single pass through Step 4 also has complexity $\mathcal{O}(npk)$. However, since Step 4 may recur, it can be shown in the absolute worst case that the number of passes is n , and worst-case complexity is $\mathcal{O}(n^2pk)$.

The number of repetitions in Steps (2-5) depends on how far from the minimum the algorithm is initialized. Near the optimum, the asymptotic convergence rate of MM algorithms is linear (De Leeuw, 1994). However, it has been shown that during the first few iterations the asymptotic linear rate does not apply, and convergence is faster (Havel, 1991).

The CCMM algorithm was coded in C++ while making extensive use of the linear algebra library *Eigen* (Guennebaud and Jacob, 2010). We used *Rcpp* (Eddelbuettel and François, 2011; Eddelbuettel, 2013; Eddelbuettel and Balamuta, 2017) to interface the program with the programming language R and *pybind11* (Jakob et al., 2017) to interface it with Python.¹ A key factor in scalability is sparsity in the weights as defined in (4). To efficiently find the k nearest neighbors of each object, we enlisted a k -d tree (Bentley, 1975) implemented by Arya et al. (2019) and Pedregosa et al. (2011).

4. Numerical Experiments

In this section, we present results of several numerical experiments. The main contribution of our research is an algorithm that performs convex clustering more efficiently than prior published algorithms. Therefore, we first present a comparison between CCMM versus its main competitors. All computational results in this paper were obtained using a desktop featuring an AMD Ryzen 5 2600X processor at 3.6 GHz using 16 GB of memory running Ubuntu version 20.04.1.

4.1 Simulated Data

To be competitive, CCMM should minimize (2) faster than state-of-the-art convex clustering algorithms including, to our knowledge, today's fastest approach: SSNAL (Sun et al., 2021). Beyond comparing CCMM to SSNAL, we consider AMA (Chi and Lange, 2015), which is available as an R-package.²

For our contest of three algorithms, we chose an approach similar to that described in Sun et al. (2021). Data sets ranging from 1,000 to 5,000 objects were generated per the two interlocking half-moons data generating process (see Figure 2). For each value of n , we used ten different realizations of the data. Since AMA and SSNAL typically minimize the unscaled loss in (1), we adjusted the scaling constants in CCMM so that each algorithm minimized the same problem. Additionally, as the software package of SSNAL does not allow for custom (connected) weight matrices, we used the weights from (3) without the scaling component, opting to set $\phi = 2$ and $k = 15$. The final input common to the three algorithms was the sequence for λ that describes the clusterpath, set to $\{0.0, 0.2, \dots, 109.8, 110.0\}$.

1. Software packages that implement CCMM for both R and Python are available at <https://github.com/djwtouw/CCMMR> and <https://github.com/djwtouw/CCMMPy>.
2. The source code for AMA can be found at <https://cran.r-project.org/src/contrib/Archive/cvxclustr/> and the source code for SSNAL at <https://blog.nus.edu.sg/mattohkc/softwares/convexclustering/>. Additionally, the code to generate the results presented in this section is available at <https://github.com/djwtouw/CCMM-paper>.

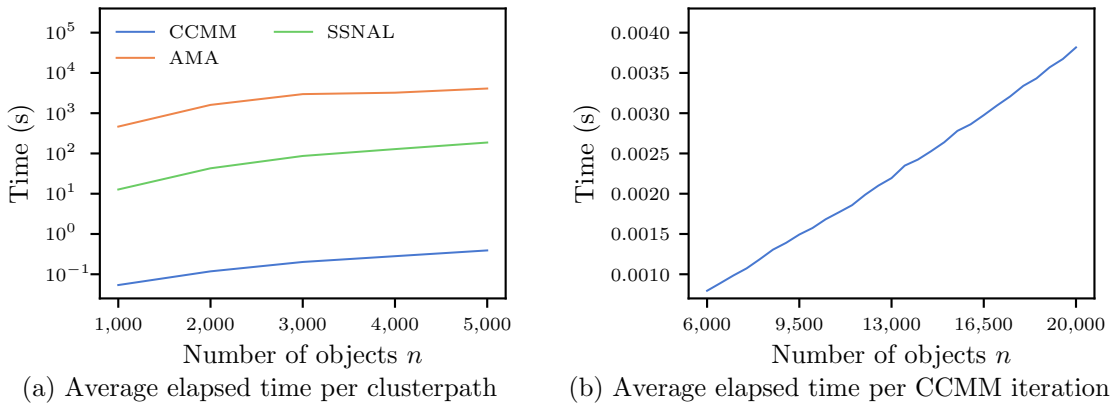


Figure 4: In Panel (a): the mean computation times for performing convex clustering on the two interlocking half moon data for the number of objects ranging from 1,000 to 5,000. In Panel (b): the mean computation time per iteration of the CCMM algorithm for the two interlocking half moons ranging from 6,000 to 20,000 objects.

For the CCMM algorithm, we set ε_c to 10^{-6} and b to 25, computing ε_f according to (11) with $\tau = 10^{-3}$. For AMA, the default tolerance for convergence of 10^{-3} was used along with the default step size parameter ν (which depends on \mathbf{W} and n). For parameters in the SSNAL algorithm, we applied default values provided by the authors. The tolerance for terminating the algorithm was set to 10^{-6} . For warm starts, 50 ADMM iterations were used for the first value for λ and 20 iterations for subsequent values.

In Figure 4a, we present mean elapsed times obtained experimentally. Results show that for $n = 1,000$, CCMM was roughly 8,610 times faster than AMA and 236 times faster than SSNAL. For $n = 5,000$, speed factors rose to 10,486 and 478 times, respectively. This convincingly proves that CCMM is the fastest algorithm to perform convex clustering. For Figure 4b, we continued the analysis of the two half-moon data sets for n ranging from 6,000 to 20,000 using only CCMM. The figure shows the average elapsed time per minimization iteration. Even though we derived in Section 3.3 each iteration's theoretical worst-case complexity to be $\mathcal{O}(n^2pk)$, we observe a trend linear in n .

To be a viable alternative to SSNAL, a new algorithm should not only minimize the loss function in less time, but also yield a similar solution. To assess the solution quality of AMA, SSNAL and CCMM, we compared values of the loss function that each algorithm obtained for data sets comprising 1,000 and 5,000 objects. In Figure 5, we use the SSNAL output as a benchmark for reporting the relative values obtained by AMA and CCMM. Being the slowest, AMA also incurs the largest values for minimizations of (1). As Figure 5b shows, the relative quality of the minimum obtained by AMA is marred by the sample size, while this is not the case for CCMM. The minimum attained by CCMM deviates at most 0.01% from that attained by SSNAL for both $n = 1,000$ and $n = 5,000$.

4.2 Empirical Data

Besides simulated data, we used several empirical data sets to compare the three algorithms: the banknotes authentication, musk and MAGIC gamma telescope data sets (Dua and Graff,

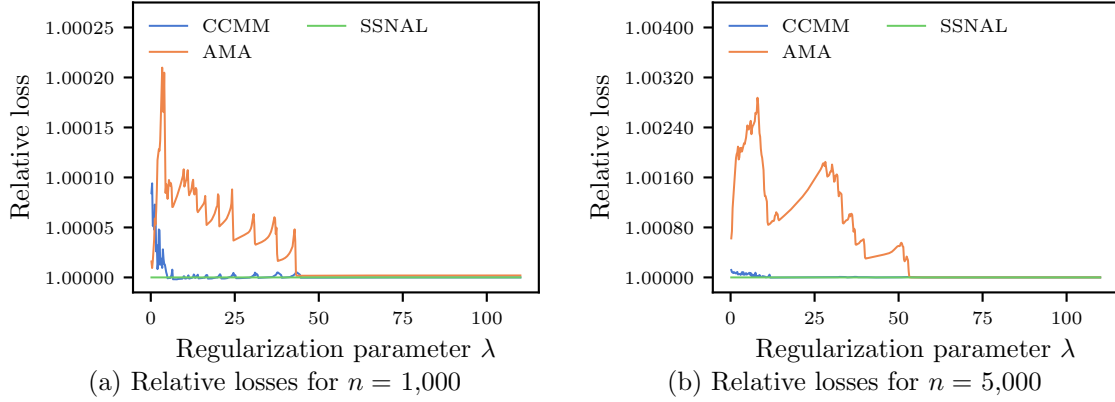


Figure 5: In Panel (a): the mean value of the loss function obtained by CCMM, SSNAL, and AMA relative to the value obtained by SSNAL. Computed for ten realizations of the two interlocking half moon data with $n = 1,000$. In Panel (b): the same as in Panel (a), but for $n = 5,000$.

Table 1: Clusterpaths for real data sets computed by three different algorithms. Dimension reduction was applied to each $n \times d$ data set using UMAP where the target number of dimensions (p) was the true number of clusters. Each clusterpath was computed for 200 values of λ that terminated at the minimum number of clusters attainable (c_{min}). This value exceeds one since the software package for SSNAL forbids the use of custom weight matrices. The three rightmost columns list the number of seconds required by each algorithm to compute the final clusterpath. A hyphen means that the algorithm was unable to complete the minimization.

	n	d	p	c_{min}	Elapsed time (s)		
					AMA	SSNAL	CCMM
Banknotes	1,372	4	2	7	402.23	51.75	0.18
Musk	6,598	166	2	27	-	197.34	0.11
Gamma	19,020	10	2	2	-	6,343.01	20.09
MNIST	60,000	784	10	6	-	-	284.43

2019), and the MNIST data set (Deng, 2012). In Table 1, the first two columns feature the number of objects (n) and variables (d) for each data set. To attain reasonable computation times, we used UMAP (McInnes et al., 2018) to reduce dimensionality to the number of categories in the data (p). Next, the weight matrices were computed using $k = 50$ and $\phi = 2$. To determine the sequence for λ , we first obtained the smallest value where the number of clusters stopped decreasing. Then, the sequence was chosen as 200 values along a cubic function from 0 to λ_{max} . Notably, omitting a symmetric circulant matrix to ensure a connected weight matrix meant that *none* of the clusterpaths terminated in a single cluster. The fourth column lists the minimum number of clusters c_{min} .

The number of seconds passed for each of the algorithms while computing the clusterpaths is reported in the three rightmost columns of Table 1. A missing result signals insufficient memory (16 GB system) for that algorithm. Results show that the speedup of CCMM over the other algorithms is dependent on the data analyzed. CCMM is about

Table 2: Variable means for the individual household electric power consumption data for the complete data set (in the leftmost column) and for the two clusters (A and B) that were found using convex clustering.

	Complete	Cluster A	Cluster B
Global active power	1.11	0.62	2.15
Global reactive power	0.12	0.11	0.13
Voltage	239.97	240.65	238.52
Global intensity	4.72	2.68	9.05
Energy sub-metering No. 1	1.18	0.63	2.35
Energy sub-metering No. 2	1.47	0.97	2.54
Energy sub-metering No. 3	5.94	0.39	17.71
Number of measurements	1,048,571	712,749	335,821

2,200 times faster than AMA for the banknotes data, which differs significantly from the results for the generated data sets. The same holds for the speedup with respect to SSNA1, which ranges from roughly 285 to almost 1,800.

4.3 Analysis of a Large Data Set

In prior sections, we have established CCMM as the most competitive algorithm to perform large-scale convex clustering. Here, we showcase CCMM analyzing a data set containing more than one million measurements of the power consumption by a single household located in Sceaux—a commune part of the Paris metropolitan area³.

Data consist of measurements sampled at one-minute intervals from the 16th of December 2006 through 16th of December 2008. Metrics include the global active and reactive power (in kilowatts), voltage (in volts), global intensity (in amperes), and the activity at three sub-metering stations (in watt-hours). The first sub-metering station monitored a kitchen, the second a laundry room, and the third a water-heater and air-conditioner. In total, there are 1,048,571 measurements, and the mean of each variable is reported in the first column of Table 2. Before performing the cluster analysis, each variable was standardized to have a mean of zero and variance of one. The weight matrix was computed using $k = 15$ and $\phi = 0.5$ in combination with the symmetric circulant matrix to ensure a complete cluster hierarchy.

For this analysis, we took an approach distinct from computing the clusterpath for a predetermined sequence for λ . While useful for comparing different algorithms, it demands advance knowledge of which value for λ maps to a specific cluster number output. For this analysis, we thus initialized λ at 0.01 and repeatedly minimized the loss function, increasing λ by 2.5% after solving each minimization. As with computing the clusterpath, the solution for the minimization problem at the prior value for λ was used as a warm start for the next value for λ . After reaching 20 clusters, the procedure entered a refinement phase. If the number of clusters was reduced by more than one as λ increased, a midpoint value was

3. The *individual household electric power consumption* data set is made available in the UCI Machine Learning Repository (Dua and Graff, 2019).

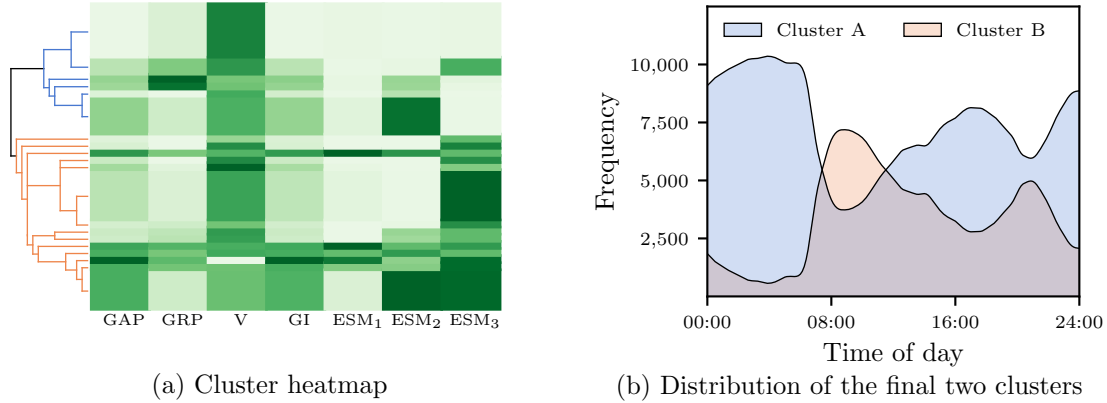


Figure 6: In Panel (a): a cluster heatmap for the final 20 clusters in the individual household electric power consumption data. The height of each row is proportional to the logarithm of the number of measurements in each of 20 clusters. Cell color is determined by the mean value of the cluster for that particular variable. In Panel (b): the distribution of timestamps in the final two clusters. Frequency is determined by the number of times each timestamp occurred in one of the clusters.

chosen to obtain a cluster hierarchy as detailed as possible. The procedure was terminated after reaching two clusters since the final reduction in cluster number is trivial. In total, 984 instances of the convex-clustering loss function were solved. The entire procedure was completed in 19.1 hours, thus solving each instance in 70 seconds, on average. To our knowledge, this is the largest data set analyzed to date via convex clustering.

In Figure 6a, a dendrogram in combination with a cluster heatmap shows the agglomeration of the final 20 clusters. Since these clusters are of different sizes, the height of each cell row in the heatmap is proportional to the logarithm of the size of the corresponding cluster. Fifteen of the final twenty clusters contain two or fewer measurements, and the largest two combined comprise over 95% of the data. The heatmap distinguishes these final two clusters by the measurements at the third energy sub-metering station. Looking at the descriptive statistics of the final two clusters in the second and third columns of Table 2, we can conclude that cluster A corresponds to measurements of lower power consumption, B to greater consumption.

To gain further insight into the final two clusters, Figure 6b shows the timestamp frequency for both clusters. Energy consumption is generally low during nighttime when members of the household are likely sleeping. Around 08:00 and 20:00, peaks emerge for cluster B to indicate general times of day that people are home, activating the heater or air-conditioner, or performing tasks like cooking or laundering. It should be noted that household members may stick to different time schedules in their power usage activities during weekends, holidays, and changing seasons. Still, this figure conveys a dense level of information about how this household generally spends its days.

5. Conclusion

In this paper, we propose a new, efficient algorithm to minimize the convex clustering loss function and compute the clusterpath. We suggest using a connected, sparse weight matrix

in combination with cluster fusions to guarantee a complete cluster hierarchy. At the heart of our minimization algorithm, which we call CCMM, lies an efficient update derived using majorization-minimization.

Our experiments show that CCMM is up to 10,486 times faster than AMA and up to 478 times faster than SSNAL while losing, at most, 0.01% accuracy. Furthermore, we analyzed a data set featuring over one million measurements of the electric power consumption by a single household. On average, solving each instance of (2) for a particular value for λ took 70 seconds. To our knowledge, this data set is the largest ever clustered using convex clustering.

One useful future research path may merge CCMM and *convex clustering via algorithmic regularization paths* (CARP). Originally developed by Weylandt et al. (2020), CARP uses small increments in the regularization parameter to compute a highly detailed clusterpath. For each value of λ , its prior solution is used as a warm start, and an ADMM algorithm (Boyd et al., 2011) is allowed to perform one iteration. In their paper, the authors showed that if the increments in λ are small enough, the difference between the results of CARP and the exact solution approaches zero. Given the efficiency of CCMM, we expect that this could suitably replace the ADMM update in CARP.

In sum, CCMM is an algorithm scaling better than state-of-the-art implementations designed to perform convex clustering. Its excellent scalability facilitates the analysis of larger data sets in less time than possible to date.

Appendix A.

In this appendix, we prove that the convex clustering loss function (2) is strongly convex.

Proof Let \mathbf{A} and \mathbf{B} be points in the domain of the convex clustering loss function L and $t \in [0, 1]$. To prove the strong convexity (see, e.g., Nesterov, 2004), we need to show that there exists $m > 0$ such that

$$tL(\mathbf{A}) + (1 - t)L(\mathbf{B}) - L(t\mathbf{A} + (1 - t)\mathbf{B}) \geq \frac{1}{2}mt(1 - t)\|\mathbf{A} - \mathbf{B}\|^2. \quad (12)$$

The left-hand side (LHS) of (12) can be rewritten as

$$\begin{aligned} \text{LHS} &= \kappa_\epsilon(t\|\mathbf{X} - \mathbf{A}\|^2 + (1 - t)\|\mathbf{X} - \mathbf{B}\|^2 - \|\mathbf{X} - t\mathbf{A} - (1 - t)\mathbf{B}\|^2) \\ &\quad + \lambda\kappa_{\text{pen}} \sum_{i < j} w_{ij} (t\|\mathbf{a}_i - \mathbf{a}_j\| + (1 - t)\|\mathbf{b}_i - \mathbf{b}_j\| - \|t(\mathbf{a}_i - \mathbf{a}_j) + (1 - t)(\mathbf{b}_i - \mathbf{b}_j)\|) \\ &= \kappa_\epsilon t(1 - t)\|\mathbf{A} - \mathbf{B}\|^2 \\ &\quad + \lambda\kappa_{\text{pen}} \sum_{i < j} w_{ij} (t\|\mathbf{a}_i - \mathbf{a}_j\| + (1 - t)\|\mathbf{b}_i - \mathbf{b}_j\| - \|t(\mathbf{a}_i - \mathbf{a}_j) + (1 - t)(\mathbf{b}_i - \mathbf{b}_j)\|). \end{aligned}$$

By the triangle inequality, the second term is greater or equal to zero. Therefore, (12) holds with $m > 0$ if the normalization constant $\kappa_\epsilon > 0$. ■

Appendix B.

This appendix contains the proof of the following theorem from Section 2.3:

Theorem 1 *If \mathbf{W} is connected, then for some sufficiently large, finite value of λ , a global minimum of (2) exists where all rows of the solution \mathbf{A} are identical to the mean of the rows in \mathbf{X} .*

Proof The point of interest is the location where the penalty term is equal to zero. This is the case if $\mathbf{a}_i = \mathbf{a}_j$ for each $w_{ij} > 0$. In this stage of the proof, the actual value of the rows is not of interest yet, only the fact that they are identical. Note that the penalty on the differences between the rows of \mathbf{A} has a nondifferentiable point if at least one of the distances is zero. To shorten notation, consider the following definition for the penalty term

$$P(\mathbf{A}) = \kappa_{\text{pen}} \sum_{i < j} w_{ij} \|\mathbf{a}_i - \mathbf{a}_j\|.$$

For the first stage, let $\hat{\mathbf{A}}$ be any value for \mathbf{A} such that $P(\hat{\mathbf{A}}) = 0$. Let the $n \times p$ matrix Σ be a deviation from $\hat{\mathbf{A}}$ under two restrictions. First, Σ must satisfy $P(\Sigma) \neq 0$ and second, we only consider values for Σ such that

$$\begin{aligned} \kappa_\epsilon \|\mathbf{X} - \mathbf{A}\|^2 &> \kappa_\epsilon \|\mathbf{X} - (\mathbf{A} + \Sigma)\|^2 \\ \text{tr}(\mathbf{X} - \hat{\mathbf{A}})^\top (\mathbf{X} - \hat{\mathbf{A}}) &> \text{tr}(\mathbf{X} - \hat{\mathbf{A}} - \Sigma)^\top (\mathbf{X} - \hat{\mathbf{A}} - \Sigma) \\ \text{tr}(\mathbf{X} - \hat{\mathbf{A}})^\top (\mathbf{X} - \hat{\mathbf{A}}) &> \text{tr}(\mathbf{X} - \hat{\mathbf{A}})^\top (\mathbf{X} - \hat{\mathbf{A}}) - 2 \text{tr}(\mathbf{X} - \hat{\mathbf{A}})^\top \Sigma + \text{tr} \Sigma^\top \Sigma \\ \text{tr}(\mathbf{X} - \hat{\mathbf{A}})^\top \Sigma &> \frac{1}{2} \text{tr} \Sigma^\top \Sigma. \end{aligned}$$

The motivation for this second restriction is that the deviation must decrease the first term of the loss function in (2). As the first restriction causes the penalty term to increase, a choice for Σ that also increases the first term surely increases the entire loss. Given that we are investigating the location of the minimum of the loss function, choices for Σ that do not satisfy the second restriction are not of interest. The following shows that for any combination of $\hat{\mathbf{A}}$ and Σ there exists a finite value for λ such that the loss corresponding to $\hat{\mathbf{A}}$ is lower than the loss corresponding to $\hat{\mathbf{A}} + \Sigma$

$$\begin{aligned} L(\hat{\mathbf{A}}) &< L(\hat{\mathbf{A}} + \Sigma) \\ \kappa_\epsilon \text{tr}(\mathbf{X} - \hat{\mathbf{A}})^\top (\mathbf{X} - \hat{\mathbf{A}}) &< \kappa_\epsilon \text{tr}(\mathbf{X} - \hat{\mathbf{A}} - \Sigma)^\top (\mathbf{X} - \hat{\mathbf{A}} - \Sigma) + \lambda P(\Sigma) \\ \kappa_\epsilon (2 \text{tr} \Sigma^\top (\mathbf{X} - \hat{\mathbf{A}}) - \text{tr} \Sigma^\top \Sigma) &< \lambda P(\Sigma) \\ \lambda &> \kappa_\epsilon \frac{2 \text{tr} \Sigma^\top (\mathbf{X} - \hat{\mathbf{A}}) - \text{tr} \Sigma^\top \Sigma}{P(\Sigma)}. \end{aligned}$$

The two restrictions imposed on Σ ensure that the resulting bound for λ is positive and that there is no division by zero. This result shows that for any $\hat{\mathbf{A}}$, there exists a value for λ such that a deviation for which the penalty term of the loss does not equal zero results in a higher loss.

The next step is to show that the $\hat{\mathbf{A}}$ that minimizes the loss in (2) is equal to $\mathbf{1}\bar{\mathbf{x}}^\top$. In order to show this, we first impose the restriction that \mathbf{W} is connected such that $P(\hat{\mathbf{A}}) = 0$

if and only if all rows of $\hat{\mathbf{A}}$ are identical. As the previous part of the proof shows that there exists a finite value for λ such that any deviation Σ from any $\hat{\mathbf{A}}$ yields a higher value for the loss, the minimum of the loss function must satisfy $P(\mathbf{A}) = 0$. Therefore, to find the minimum we now minimize

$$L(\hat{\mathbf{A}}) = \kappa_\epsilon \sum_{i=1}^n \|\mathbf{x}_i - \hat{\mathbf{a}}\|^2,$$

for which the solution is $\hat{\mathbf{a}} = \frac{1}{n} \sum_{i=1}^n \mathbf{x}_i = \bar{\mathbf{x}}$. This completes the proof that for a connected weight matrix \mathbf{W} , the minimum of (2) for a sufficiently large value for λ is attained at $\mathbf{A} = \mathbf{1}\bar{\mathbf{x}}^\top$. \blacksquare

Appendix C.

This appendix contains the proof of the following theorem from Section 3.1:

Theorem 3 *Let the matrix \mathbf{M} contain the c unique rows of \mathbf{A} , and let ε_f be the threshold used for fusing rows of \mathbf{M} . Assume that $\|\mathbf{m}_k - \mathbf{m}_l\| \leq \varepsilon_f$ for some $k \neq l$. Let \mathbf{m}_{new} be the weighted average of \mathbf{m}_k and \mathbf{m}_l computed as in (5), and let \mathbf{M}_{new} be the matrix that results from setting \mathbf{m}_k and \mathbf{m}_l to \mathbf{m}_{new} . Then, for fixed λ and \mathbf{W} , the absolute error $|L(\mathbf{M}) - L(\mathbf{M}_{new})|$ tends toward zero as $\varepsilon_f \rightarrow 0$.*

Proof If $\|\mathbf{m}_k - \mathbf{m}_l\| \leq \varepsilon_f$, the new cluster centroid is computed as in (5). Let

$$\begin{aligned} \boldsymbol{\sigma}_k &= \mathbf{m}_k - \mathbf{m}_{new} = \frac{|C_l|}{|C_k| + |C_l|} (\mathbf{m}_k - \mathbf{m}_l) \\ \boldsymbol{\sigma}_l &= \mathbf{m}_l - \mathbf{m}_{new} = \frac{|C_k|}{|C_k| + |C_l|} (\mathbf{m}_l - \mathbf{m}_k), \end{aligned}$$

such that

$$\|\boldsymbol{\sigma}_k\| \leq \frac{|C_l|}{|C_k| + |C_l|} \varepsilon_f \quad \text{and} \quad \|\boldsymbol{\sigma}_l\| \leq \frac{|C_k|}{|C_k| + |C_l|} \varepsilon_f. \quad (13)$$

Writing out the absolute value of the difference between the loss before and after merging \mathbf{m}_k and \mathbf{m}_l , we obtain

$$\begin{aligned} |L(\mathbf{M}) - L(\mathbf{M}_{new})| &= \left| \kappa_\epsilon \left(\sum_{i \in C_k} \|\mathbf{x}_i - \mathbf{m}_k\|^2 + \sum_{i \in C_l} \|\mathbf{x}_i - \mathbf{m}_l\|^2 \right. \right. \\ &\quad \left. \left. - \sum_{i \in C_k} \|\mathbf{x}_i - \mathbf{m}_{new}\|^2 - \sum_{i \in C_l} \|\mathbf{x}_i - \mathbf{m}_{new}\|^2 \right) \right. \\ &\quad \left. + \lambda \kappa_{\text{pen}} \left(\sum_{\substack{i=0 \\ i \notin \{k,l\}}}^c \mathbf{u}_k^\top \mathbf{W} \mathbf{u}_i \|\mathbf{m}_k - \mathbf{m}_i\| \right. \right. \\ &\quad \left. \left. + \sum_{\substack{i=0 \\ i \notin \{k,l\}}}^c \mathbf{u}_l^\top \mathbf{W} \mathbf{u}_i \|\mathbf{m}_l - \mathbf{m}_i\| + \mathbf{u}_k^\top \mathbf{W} \mathbf{u}_l \|\mathbf{m}_k - \mathbf{m}_l\| \right) \right| \end{aligned}$$

$$- \sum_{\substack{i=0 \\ i \notin \{k, l\}}}^c \mathbf{u}_k^\top \mathbf{W} \mathbf{u}_i \|\mathbf{m}_{new} - \mathbf{m}_i\| - \sum_{\substack{i=0 \\ i \notin \{k, l\}}}^c \mathbf{u}_l^\top \mathbf{W} \mathbf{u}_i \|\mathbf{m}_{new} - \mathbf{m}_i\| \Bigg) \Bigg|,$$

where the first two lines concern the difference between the first terms of $L(\mathbf{M})$ and $L(\mathbf{M}_{new})$ and the remaining three lines concern the difference between the values of the penalty terms. Using the triangle inequality, this can be written as

$$|L(\mathbf{M}) - L(\mathbf{M}_{new})| \leq \kappa_\epsilon |\Gamma_1| + \lambda \kappa_{\text{pen}} |\Gamma_2|,$$

where Γ_1 is the result of the terms on the first two lines and Γ_2 is the result of the terms on the remaining four lines. We start by providing an upper bound for $|\Gamma_1|$. Rewriting yields

$$\begin{aligned} |\Gamma_1| &= \left| \sum_{i \in C_k} (\|\mathbf{x}_i - \mathbf{m}_k\|^2 - \|\mathbf{x}_i - \mathbf{m}_{new}\|^2) + \sum_{i \in C_l} (\|\mathbf{x}_i - \mathbf{m}_l\|^2 - \|\mathbf{x}_i - \mathbf{m}_{new}\|^2) \right| \\ &= \left| \sum_{i \in C_k} (\|\mathbf{x}_i - \mathbf{m}_k\|^2 - \|\mathbf{x}_i - \mathbf{m}_k + \boldsymbol{\sigma}_k\|^2) + \sum_{i \in C_l} (\|\mathbf{x}_i - \mathbf{m}_l\|^2 - \|\mathbf{x}_i - \mathbf{m}_l + \boldsymbol{\sigma}_l\|^2) \right| \\ &= \left| \sum_{i \in C_k} (\boldsymbol{\sigma}_k^\top \boldsymbol{\sigma}_k - 2(\mathbf{x}_i - \mathbf{m}_k)^\top \boldsymbol{\sigma}_k) + \sum_{i \in C_l} (\boldsymbol{\sigma}_l^\top \boldsymbol{\sigma}_l - 2(\mathbf{x}_i - \mathbf{m}_l)^\top \boldsymbol{\sigma}_l) \right|, \end{aligned}$$

which is bounded by

$$\begin{aligned} |\Gamma_1| &\leq \sum_{i \in C_k} (\boldsymbol{\sigma}_k^\top \boldsymbol{\sigma}_k + 2|(\mathbf{x}_i - \mathbf{m}_k)^\top \boldsymbol{\sigma}_k|) + \sum_{i \in C_l} (\boldsymbol{\sigma}_l^\top \boldsymbol{\sigma}_l + 2|(\mathbf{x}_i - \mathbf{m}_l)^\top \boldsymbol{\sigma}_l|) \\ &\leq \sum_{i \in C_k} (\boldsymbol{\sigma}_k^\top \boldsymbol{\sigma}_k + 2\|\mathbf{x}_i - \mathbf{m}_k\| \|\boldsymbol{\sigma}_k\|) + \sum_{i \in C_l} (\boldsymbol{\sigma}_l^\top \boldsymbol{\sigma}_l + 2\|\mathbf{x}_i - \mathbf{m}_l\| \|\boldsymbol{\sigma}_l\|) \\ &\leq \frac{|C_k| |C_l|}{|C_k| + |C_l|} \varepsilon_f^2 + \frac{2}{|C_k| + |C_l|} \left(|C_l| \sum_{i \in C_k} \|\mathbf{x}_i - \mathbf{m}_k\| + |C_k| \sum_{i \in C_l} \|\mathbf{x}_i - \mathbf{m}_l\| \right) \varepsilon_f, \end{aligned}$$

where we made use of the triangle inequality, the Cauchy-Schwarz inequality, and (13). Each of the terms in the upper bound is now proportional to ε_f . To bound $|\Gamma_2|$, consider

$$\begin{aligned} \|\mathbf{m}_k - \mathbf{m}_i\| - \|\mathbf{m}_{new} - \mathbf{m}_i\| &= \|\mathbf{m}_k - \mathbf{m}_i\| - \|\mathbf{m}_k - \boldsymbol{\sigma}_k - \mathbf{m}_i\| \\ &= \|\boldsymbol{\sigma}_k + \mathbf{m}_k - \boldsymbol{\sigma}_k - \mathbf{m}_i\| - \|\mathbf{m}_k - \boldsymbol{\sigma}_k - \mathbf{m}_i\|, \end{aligned}$$

and by means of the triangle inequality we obtain

$$\begin{aligned} \|\boldsymbol{\sigma}_k + \mathbf{m}_k - \boldsymbol{\sigma}_k - \mathbf{m}_i\| &\leq \|\boldsymbol{\sigma}_k\| + \|\mathbf{m}_k - \boldsymbol{\sigma}_k - \mathbf{m}_i\| \\ \|\mathbf{m}_k - \mathbf{m}_i\| - \|\mathbf{m}_k - \boldsymbol{\sigma}_k - \mathbf{m}_i\| &\leq \|\boldsymbol{\sigma}_k\|. \end{aligned}$$

This can be combined with

$$\begin{aligned} \|\mathbf{m}_k - \boldsymbol{\sigma}_k - \mathbf{m}_i\| &\leq \|\mathbf{m}_k - \mathbf{m}_i\| + \|\boldsymbol{\sigma}_k\| \\ \|\mathbf{m}_k - \boldsymbol{\sigma}_k - \mathbf{m}_i\| - \|\mathbf{m}_k - \mathbf{m}_i\| &\leq \|\boldsymbol{\sigma}_k\|, \end{aligned}$$

to obtain

$$\left| \|\mathbf{m}_k - \mathbf{m}_i\| - \|\mathbf{m}_{new} - \mathbf{m}_i\| \right| \leq \|\boldsymbol{\sigma}_k\|. \quad (14)$$

The upper bound for $|\Gamma_2|$ is

$$\begin{aligned} |\Gamma_2| &= \left| \sum_{\substack{i=0 \\ i \notin \{k,l\}}}^c \mathbf{u}_k^\top \mathbf{W} \mathbf{u}_i (\|\mathbf{m}_k - \mathbf{m}_i\| - \|\mathbf{m}_{new} - \mathbf{m}_i\|) \right. \\ &\quad \left. + \sum_{\substack{i=0 \\ i \notin \{k,l\}}}^c \mathbf{u}_l^\top \mathbf{W} \mathbf{u}_i (\|\mathbf{m}_l - \mathbf{m}_i\| - \|\mathbf{m}_{new} - \mathbf{m}_i\|) + \mathbf{u}_k^\top \mathbf{W} \mathbf{u}_l \|\mathbf{m}_k - \mathbf{m}_l\| \right| \\ &\leq \sum_{\substack{i=0 \\ i \notin \{k,l\}}}^c \mathbf{u}_k^\top \mathbf{W} \mathbf{u}_i \|\boldsymbol{\sigma}_k\| + \sum_{\substack{i=0 \\ i \notin \{k,l\}}}^c \mathbf{u}_l^\top \mathbf{W} \mathbf{u}_i \|\boldsymbol{\sigma}_l\| + \mathbf{u}_k^\top \mathbf{W} \mathbf{u}_l \|\mathbf{m}_k - \mathbf{m}_l\| \\ &\leq \left(\mathbf{u}_k^\top \mathbf{W} \mathbf{u}_l + \frac{|C_l|}{|C_k| + |C_l|} \sum_{\substack{i=0 \\ i \notin \{k,l\}}}^c \mathbf{u}_k^\top \mathbf{W} \mathbf{u}_i + \frac{|C_k|}{|C_k| + |C_l|} \sum_{\substack{i=0 \\ i \notin \{k,l\}}}^c \mathbf{u}_l^\top \mathbf{W} \mathbf{u}_i \right) \varepsilon_f, \end{aligned}$$

where we made use of the triangle inequality, (13), and (14). From these two upper bounds, we can conclude that if $\varepsilon_f \rightarrow 0$, both $|\Gamma_1| \rightarrow 0$ and $|\Gamma_2| \rightarrow 0$. Hence, $|L(\mathbf{M}) - L(\mathbf{M}_{new})| \rightarrow 0$ as $\varepsilon_f \rightarrow 0$. \blacksquare

References

S. Arya, D. Mount, S. E. Kemp, and G. Jefferis. *RANN: Fast Nearest Neighbour Search (Wraps ANN Library) Using L2 Metric*, 2019. URL <https://CRAN.R-project.org/package=RANN>. R package version 2.6.1.

J. L. Bentley. Multidimensional Binary Search Trees Used for Associative Searching. *Communications of the ACM*, 18(9):509–517, 1975.

S. P. Boyd and L. Vandenberghe. *Convex Optimization*. Cambridge University Press, 2004.

S. P. Boyd, N. Parikh, E. Chu, B. Peleato, and J. Eckstein. Distributed Optimization and Statistical Learning via the Alternating Direction Method of Multipliers. *Foundations and Trends® in Machine learning*, 3(1):1–122, 2011.

R. Bronson. *Schaum's Outline of Theory and Problems of Matrix Operations*. McGraw-Hill, 1989.

E. C. Chi and K. L. Lange. Splitting Methods for Convex Clustering. *Journal of Computational and Graphical Statistics*, 24(4):994–1013, 2015.

L. Deng. The MNIST Database of Handwritten Digit Images for Machine Learning Research. *IEEE Signal Processing Magazine*, 29(6):141–142, 2012.

D. Dua and C. Graff. UCI Machine Learning Repository, 2019. URL <http://archive.ics.uci.edu/ml>.

D. Eddelbuettel. *Seamless R and C++ Integration with Rcpp*. Springer, 2013.

D. Eddelbuettel and J. J. Balamuta. Extending R with C++: A Brief Introduction to Rcpp. *PeerJ Preprints*, 5:e3188v1, 2017.

D. Eddelbuettel and R. François. Rcpp: Seamless R and C++ Integration. *Journal of Statistical Software*, 40(8):1–18, 2011.

G. Gan, C. Ma, and J. Wu. *Data Clustering: Theory, Algorithms, and Applications*. SIAM, 2007.

J. C. Gower and P. J. F. Groenen. Applications of the Modified Leverrier-Faddeev Algorithm for the Construction of Explicit Matrix Spectral Decompositions and Inverses. *Utilitas Mathematica*, 40:51–64, 1991.

P. J. F. Groenen, W. J. Heiser, and J. J. Meulman. Global Optimization in Least Squares Multidimensional Scaling by Distance Smoothing. *Journal of Classification*, 16(2):225–254, 1999.

G. Guennebaud and B. Jacob. Eigen v3. <http://eigen.tuxfamily.org>, 2010.

T. F. Havel. An Evaluation of Computational Strategies for Use in the Determination of Protein Structure from Distance Constraints Obtained by Nuclear Magnetic Resonance. *Progress in Biophysics and Molecular Research*, 56(1):43–78, 1991.

T. D. Hocking, A. Joulin, F. Bach, and J.-P. Vert. Clusterpath: An Algorithm for Clustering Using Convex Fusion Penalties. In *The 28th International Conference on Machine Learning*, Bellevue, Washington, 2011.

D. R. Hunter and K. L. Lange. A Tutorial on MM Algorithms. *The American Statistician*, 58(1):30–37, 2004.

W. Jakob, J. Rhinelander, and D. Moldovan. pybind11—Seamless operability between C++11 and Python, 2017. <https://github.com/pybind/pybind11>.

K. L. Lange, D. R. Hunter, and I. Yang. Optimization Transfer Using Surrogate Objective Functions. *Journal of Computational and Graphical Statistics*, 9(1):1–20, 2000.

J. Leeuw, de. Applications of Convex Analysis to Multidimensional Scaling. In J.-R. Barra, F. cois Brodeau, G. Romier, and B. van Cutsem, editors, *Recent Developments in Statistics*, pages 133–146. North Holland Publishing Company, 1977.

J. Leeuw, de. Block-Relaxation Algorithms in Statistics. In H.-H. Bock, W. Lenski, and M. M. Richter, editors, *Information Systems and Data Analysis*, pages 308–324. Springer Berlin Heidelberg, 1994.

J. Leeuw, de and W. J. Heiser. Multidimensional Scaling with Restrictions on the Configuration. *Multivariate Analysis*, 5(1):501–522, 1980.

F. Lindsten, H. Ohlsson, and L. Ljung. Just Relax and Come Clustering!: A Convexification of K-Means Clustering. Technical report, Department of Electrical Engineering, Linköping University, Linköping, Sweden, 2011.

J. MacQueen. Some Methods for Classification and Analysis of Multivariate Observations. In *Proceedings of the Fifth Berkeley Symposium on Mathematical Statistics and Probability*, pages 281–297, 1967.

L. McInnes, J. Healy, and J. Melville. UMAP: Uniform Manifold Approximation and Projection for Dimension Reduction, 2018. URL <https://arxiv.org/abs/1802.03426>.

Y. Nesterov. *Introductory Lecture on Convex Optimization: A Basic Course*. Springer New York, 2004.

J. M. Ortega and W. C. Rheinboldt. *Iterative Solution of Nonlinear Equations in Several Variables*. Academic Press, 1970.

F. Pedregosa, G. Varoquaux, A. Gramfort, V. Michel, B. Thirion, O. Grisel, M. Blondel, P. Prettenhofer, R. Weiss, V. Dubourg, J. Vanderplas, A. Passos, D. Cournapeau, M. Brucher, M. Perrot, and E. Duchesnay. Scikit-learn: Machine Learning in Python. *Journal of Machine Learning Research*, 12:2825–2830, 2011.

K. Pelckmans, J. de Brabanter, J. A. K. Suykens, and B. de Moor. Convex Clustering Shrinkage. In *PASCAL Workshop on Statistics and Optimization of Clustering Workshop*, 2005.

D. Sun, K.-C. Toh, and Y. Yuan. Convex Clustering: Model, Theoretical Guarantee and Efficient Algorithm. *Journal of Machine Learning Research*, 22(9):1–32, 2021.

H. Voß and U. Eckhardt. Linear Convergence of Generalized Weiszfeld’s Method. *Computing*, 25(3):243–251, 1980.

E. Weiszfeld. Sur le Point pour lequel la Somme des Distances de n Points Donnés Est Minimum. *Tohoku Mathemacial Journal*, 43:355–386, 1937.

M. Weylandt, J. Nagorski, and G. I. Allen. Dynamic Visualization and Fast Computation for Convex Clustering via Algorithmic Regularization. *Journal of Computational and Graphical Statistics*, 29(1):87–96, 2020.

M. Yuan and Y. Lin. Model Selection and Estimation in Regression with Grouped Variables. *Journal of the Royal Statistical Society: Series B (Statistical Methodology)*, 68(1):49–67, 2006.

A. L. Yuille and A. Rangarajan. The Concave-Convex Procedure. *Neural Computation*, 15(4):915–936, 2003.